TU Delft

Delft University of Technology

Metatranscriptomics provides an in-depth perspective on the resistance and detoxification of anammox bacteria to dissolved oxygen in a pilot CANON process

Xu, Huaihao; Wang, Xiaojun; Wang, Mingyuan; Wu, Junbin; Zhang, Bo; Wang, Jinsong; Zhang, Qiuting; Lin, Bingrong; Chen, Shaohua

DOI
10.1016/j.watres.2024.122613

Publication date
2025

Document Version
Final published version

Published in
Water Research

Citation (APA)
Xu, H., Wang, X., Wang, M., Wu, J., Zhang, B., Wang, J., Zhang, Q., Lin, B., & Chen, S. (2025). Metatranscriptomics provides an in-depth perspective on the resistance and detoxification of anammox bacteria to dissolved oxygen in a pilot CANON process. *Water Research*, *268*, Article 122613. https://doi.org/10.1016/j.watres.2024.122613

Important note
To cite this publication, please use the final published version (if applicable).
Please check the document version above.

Copyright
Other than for strictly personal use, it is not permitted to download, forward or distribute the text or part of it, without the consent of the author(s) and/or copyright holder(s), unless the work is under an open content license such as Creative Commons.

Takedown policy
Please contact us and provide details if you believe this document breaches copyrights.
We will remove access to the work immediately and investigate your claim.

This work is downloaded from Delft University of Technology.
For technical reasons the number of authors shown on this cover page is limited to a maximum of 10.

Green Open Access added to TU Delft Institutional Repository

'You share, we take care!' - Taverne project

https://www.openaccess.nl/en/you-share-we-take-care

Otherwise as indicated in the copyright section: the publisher is the copyright holder of this work and the author uses the Dutch legislation to make this work public.

Water Research 268 (2025) 122613

Contents lists available at ScienceDirect

Water Research

journal homepage: www.elsevier.com/locate/watres

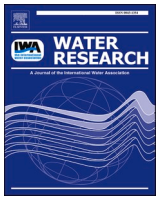

Metatranscriptomics provides an in-depth perspective on the resistance and detoxification of anammox bacteria to dissolved oxygen in a pilot CANON process

Huaihao Xu [a,b], Xiaojun Wang [a,*], Mingyuan Wang [a], Junbin Wu [a], Bo Zhang [a,b], Jinsong Wang [d], Qiuting Zhang [c], Bingrong Lin [c], Shaohua Chen [a]

[a] CAS Key Laboratory of Urban Pollutant Conversion, Institute of Urban Environment, Chinese Academy of Sciences, Xiamen 361021, PR China
[b] University of Chinese Academy of Sciences, Beijing 100049, PR China
[c] Longyan Water Environment Development Co. Ltd., Longyan 364000, PR China
[d] Department of Biotechnology, Delft University of Technology, Van der Maasweg 9 2629 HZ, Delft, The Netherlands

ARTICLE INFO

Keywords:
DO tolerance of anammox
Candidatus Kuenenia
Specific anammox activity
Metabolic regulation
oxygen detoxification

ABSTRACT

In the completely autotrophic nitrogen removal over nitrite (CANON) process, the conflicting oxygen requirements of anammox and ammonium-oxidizing bacteria often lead to retardation in anammox activity. However, our study achieved stable nitrogen removal with a maximum capacity of 1096 g-N/m^3/d in a 20 m^3 CANON reactor under long-term intensive aeration. The anammox bacteria unusually distributed in the outer layer of the biofilm and demonstrated remarkable oxygen tolerance. Their activity only declined by 18.5 % under 2.0 mg/L of dissolved oxygen. When anammox bacteria encountered oxygen exposure, they adopted some strategies. Metatranscriptomics revealed that *Candidatus Kuenenia*, the dominant anammox species in our system, downregulated its gene expressions involved in carbon metabolism and oxidative phosphorylation. This may reduce electron leakage that combines with O_2, thereby minimizing the generation of reactive oxygen species (ROS). By contrast, the secretion of extracellular proteins and conversion of $O_2^{\cdot-}$ were upregulated to eliminate ROS promptly. This behavior endowed *Ca. Kuenenia* with a unique oxygen detoxification pathway: $O_2^{\cdot-}$ were initially converted to H_2O_2 by superoxide dismutase *SOD2* and superoxide reductase *dfx* (major role), followed by reduction to H_2O via non-heme chloroperoxidase *cpo* (a newly recognized mechanism in the oxygen detoxification of anammox) and catalase *katE*. These results expanded the current knowledge of anammox alleviating oxidative stress.

1. Introduction

The Completely Autotrophic Nitrogen Removal over Nitrite (CANON) process based on anaerobic ammonium oxidation (anammox) has become an important research focus due to its advantages of energy conservation, cost reduction, and environmental friendliness (Du et al., 2022). The CANON process for biological nitrogen removal consists of the partial nitrification and anammox stages, both occurring in the same reactor (Third et al., 2001). The inherent contradiction between the oxygen demands of partial nitrification and anammox determines that dissolved oxygen (DO) is a key parameter affecting its operation. It has traditionally been believed that the suitable DO concentration for anammox bacteria is below 0.2 mg/L, which is lower than the range required for ammonia-oxidizing bacteria (AOB) to oxidize ammonia (Varas et al., 2015). Consequently, the aeration conditions in the CANON process are often complex (Wang et al., 2019), significantly increasing equipment costs and operational challenges. This complexity represents one of the bottlenecks hindering the widespread application of the CANON technology.

Anammox bacteria were initially considered obligate autotrophic anaerobes whose activity would be inhibited by the presence of DO (Mulder et al., 1995). It was later discovered that anammox bacteria and AOB could form bioaggregates (biofilms or granular sludge) and coexist synergistically. AOB occupies the outer layer of the bioaggregates and consumes oxygen, creating a low-oxygen environment and providing the substrate nitrite for the inner anammox bacteria (Ren et al., 2022).

* Corresponding author.
E-mail address: xjwang@iue.ac.cn (X. Wang).

https://doi.org/10.1016/j.watres.2024.122613
Received 16 March 2024; Received in revised form 8 October 2024; Accepted 9 October 2024
Available online 11 October 2024
0043-1354/© 2024 Elsevier Ltd. All rights are reserved, including those for text and data mining, AI training, and similar technologies.

However, a recently revealed phenomenon contradicts the previous experience. In the oxic zone of an alternating anaerobic/oxic/anoxic/oxic (AOAO) process, anammox bacteria were predominantly found in the outer layer of the biofilm on the carriers because of the abundant nitrite produced by AOB in the suspended sludge (Feng et al., 2022). At this point, substrate, instead of DO, became the primary factor governing the distribution of anammox bacteria in the biofilm. In addition, unlike obligate anaerobes such as methanogens, the inhibition of anammox bacteria by DO is reversible (Seuntjens et al., 2018). Furthermore, increasing evidence suggests that anammox bacteria possess oxygen tolerance and detoxification abilities that differ from the previous understanding.

A complete detoxification process may occur when oxygen invades into anaerobic cells, where the superoxide radicals generated from the electron gain of oxygen are sequentially reduced to H_2O_2 and H_2O initiated by superoxides enzymes (e.g., superoxide dismutase) and peroxides enzymes (e.g., catalase), respectively (Cannio et al., 2000). Despite the current inability to cultivate pure anammox bacteria, genomic techniques have provided powerful tools for further elucidating the ecological and physiological characteristics of these bacteria under oxygen exposure. For instance, Ji et al. (2019) applied metagenomic and metatranscriptomic analyses to reveal the oxygen detoxification capability of *Ca. Brocadia*, a dominated anammox culture enriched from non-strict anaerobic conditions. Moreover, an investigation on the oxygen-active proteins discovered a novel oxygen defence system in a genus *Ca. Loosdrechtia aerotolerans*, where the novel *cbb3*-type cytochrome c oxidase and bifunctional catalase-peroxidase endowed the bacteria with robust oxygen tolerance (Yang et al., 2022). Therefore, the oxygen detoxification mechanisms are likely diverse among different anammox bacteria. However, the physiological metabolism of anammox bacteria under DO stress was rarely studied in CANON process, particularly in a pilot-scale.

In this study, different levels of DO resistance were observed in anammox biomass in spatial variety within a pilot-scale CANON reactor that had been long-term operated under high DO conditions. The population and metabolic characteristics of anammox bacteria were investigated based on both metagenomics and metatranscriptomics. We identified a number of novel gene expressions in anammox, and unravel the unique response mechanism of anammox bacteria to environmental factors, especially DO, in CANON process. This study expands our fundamental understanding on the oxygen detoxification capability of anammox bacteria in CANON process.

2. Materials and methods

2.1. Source and collection of samples

The sludge samples used in this study were obtained from a long-term operational pilot-scale CANON system treating mature landfill leachate. The effective volume was 20 m^3, and the hydraulic retention time (HRT) was one day. The CANON was a hybrid system of biofilm and suspended sludge. A large amount of carriers (consisting of sponge cubes and Pall rings with a ratio of 1:2) floated on the upper of the reactor, the volume of which accounts for 50 % of the total. These carriers were in a relatively fixed position due to mutual accumulation. Below the carrier layer was a suspended sludge layer with a mixing device to mix it thoroughly. The inlet pipe passed through the carrier layer deep into the suspended sludge layer (see Fig. 1 for detailed information).

As the reactor operated, we found that the biochemical system exhibited robust anammox activity even under high-intensity aeration (8-minute aeration with 2-minute intervals as a cycle). We perfomed sampling on day 445. Three sampling sites were sequentially set along the flow path within the bioreactor. Site 1 was close to the inlet, site 2 was in the middle, and site 3 was close to the outlet (Fig. 1). The carrier layer samples (consisting of sponge cubes and Pall rings) collected from these three sampling points were named car1, car2, and car3, respectively. Suspended sludge below the carrier layer was collected using a water sampler and named susp. The sponge cubes and pall rings were sorted from car1, car2, and car3 equally and named spon and pall, respectively. A vortex oscillator was used to detach and homogenize the biomass from the carriers. The collected biomass was stored at −80 °C for DNA and RNA extraction. Additionally, a portion of the biomass was used for the quantification of extracellular polymeric substances (EPS) following the method of Zhang et al. (2022). All samples were prepared in triplicate.

Long-term monitoring of environmental factors was conducted for each sampling site. The influent and effluent of the CANON reactor were also recorded. DO measurements were performed by a portable DO meter. NH_4^+-N, NO_2^--N, and NO_3^--N were determined following the standard methods (APHA et al., 2012).

2.2. Specific anammox activity (SAA) tests under anaerobic and DO exposure conditions

Sample car1, car2, car3, and susp were collected for SAA tests (Text S1). The flasks were left open for the DO exposure experiments, and the shaker speed was set at 50, 100, or 150 rpm to provide different levels of

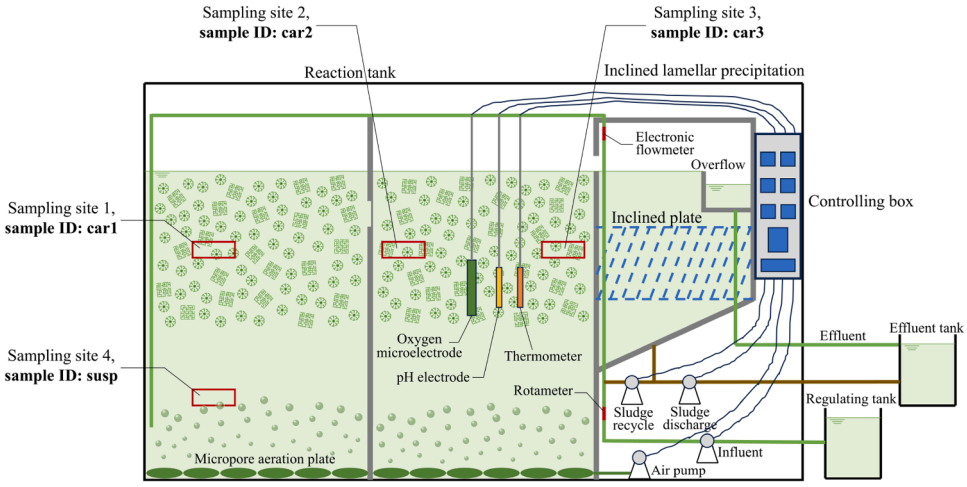

Fig. 1. Schematic diagram of the pilot CANON process. After flowing through the regulating tank, the leachate entered the reaction tank, which had the built-in thermometer, pH, and DO probes to collect real-time temperature data and regulate pH and aeration through an online control system. An inclined plate sedimentation tank was arranged at the end of the device to retain sludge.

DO exposure. The DO concentration in the reaction system was recorded every 10 min using a portable DO meter.

2.3. Metagenomics

To investigate the microbial community compositions of different types of biocarrier, sample susp, spon, and pall were used for metagenomic analysis. DNA extraction, quality control, sequencing, and library construction were conducted by Shanghai Majorbio Bio-pharm Technology Co., Ltd (Shanghai, China). Metagenomic analysis can be found in Text S2.

2.4. Metatranscriptomics

To explore the response mechanism to oxygen stress, sample susp, car1, car2, and car3 were used for metatranscriptomic analysis. RNA extraction, sequencing, and library construction were conducted by Shanghai Majorbio Bio-pharm Technology Co., Ltd (Shanghai, China). Gene abundance was based on FPKM values, which stands for Fragments Per Kilobase of exon model per Million mapped reads (Mortazavi et al., 2008). BLASTP (http://blast.ncbi.nlm.nih.gov/Blast.cgi) (Altschul et al., 1997) was utilized to compare the non-redundant gene set against the NR and KEGG database to obtain taxonomic and functional annotations, respectively. Furthermore, taxonomic and functional information was combined to offer insights into the functions expressed by a particular taxon (Montoya-Rosales et al., 2023). More information about metatranscriptomics can be found in Text S3.

2.5. Statistical analysis

Due to the varying abundance of anammox bacteria (mainly referred to *Ca. Kuenenia* in this study) across different samples, a normalization process was applied to the transcriptome data in order to compare gene expression levels on a consistent basis. Specifically, the expression abundance of a particular gene expressed by *Ca. Kuenenia* in a sample was determined by dividing the FPKM value of that gene by the total FPKM value of all genes transcribed by *Ca. Kuenenia* in the same sample, with the resulting unit being parts per million (ppm). This normalized data was subsequently used for further analysis. The software edgeR was utilized to compare the gene expression levels between two samples and identify differentially expressed genes (DEGs) (Robinson et al., 2010), with the criteria set as FDR < 0.05 and $|\log_2 FC| > 1$ (FC, Fold Change). This study selected sample susp as the control group for differential analysis. The other statistical methodologies can be found in Text S4. The error bars in the figures represent the standard deviation.

3. Results

3.1. Performances of the pilot CANON process

Our pilot-scale CANON system was operated for over one year, and the nitrogen removal performance of the bioreactor is presented in Fig. 2 (A). In Phase I, the leachate was diluted with water to prevent substrate inhibition, ensuring that the NH_4^+-N in the influent was controlled below 300 mg/L. Then the dilution of the influent was gradually reduced to increase the nitrogen load. Due to variations in the intrinsic water quality of the raw leachate, the influent NH_4^+-N in Phase II exhibited substantial fluctuations within a wide range of 106 ~ 904 mg/L, with a 488 mg/L average. Similarly, in the early operational stages, AOB responsible for partial nitrification was not effectively cultivated to match the stoichiometry of anammox. Consequently, nitrite supplementation was necessary to provide sufficient substrate for anammox. In Phase II, the amount of nitrite added was gradually reduced as AOB activity achieved 153 g-N/m^3/d averagely. It is worth mentioning that this supplementation to sustain the anammox activity was continuously dynamically adjusted, which led to some extreme NO_2^--N peaks being attributed to system malfunctions. Due to the low biodegradable organic carbon in the influent of mature leachate ($\Delta COD_{inf\text{-}eff} < 200$ mg/L), heterotrophic denitrification was overlooked and TN removal was attributed entirely to the anammox pathway. The average nitrogen removal rate increased from 247 g-N/m^3/d in Phase I to 428 g-N/m^3/d in Phase II, with extreme values reaching as high as 1096 g-N/m^3/d. Since AOB activity could not satisfy the needs of anammox process, high NH_4^+-N concentration in the effluent resulted in an average TN removal efficiency that was lower than the theoretical stoichiometry, at only 65.61 % in Phase I and 66.60 % in Phase II. The effluent of our pilot reactor was directed to a leachate treatment system operated within the landfill site for further treatment, rather than being directly discharged into the environment.

Before the formal collection of sludge samples on the 445th day, we monitored various environmental factors at each sampling site for six months, and the results are presented in Fig. 2(B). Due to the prolonged

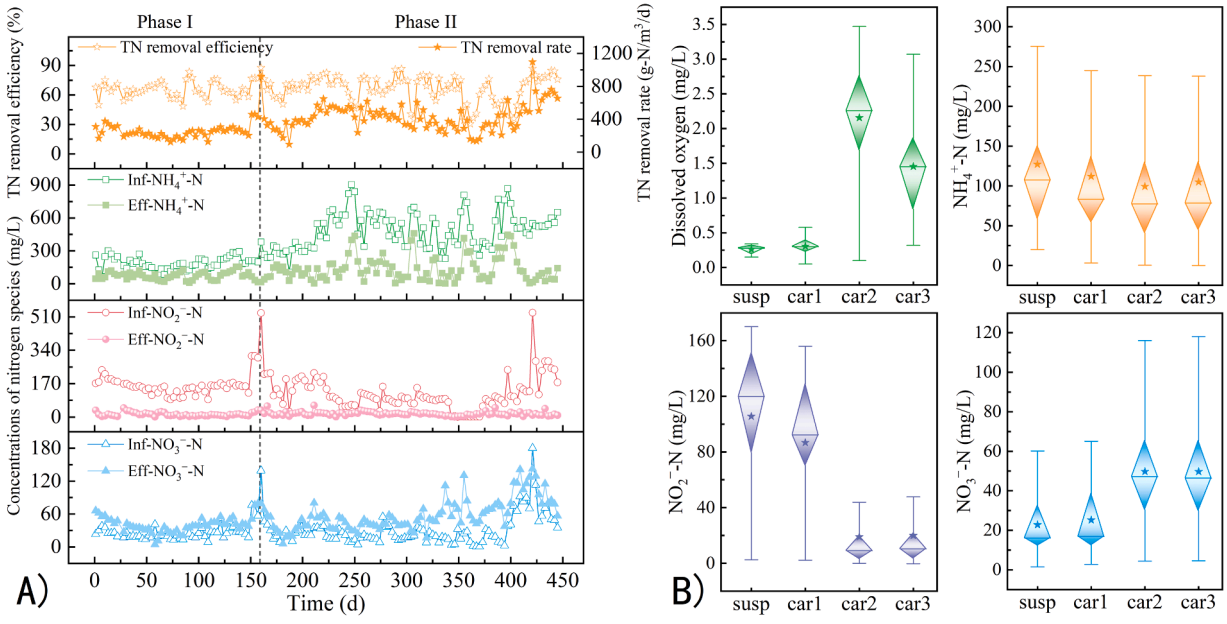

Fig. 2. Performances of the pilot CANON process: (A) Nitrogen removal capacity of the reactor; (B) Environmental factors of each sampling site in the reaction tank.

suboptimal activity of partial nitrification in the CANON process, a relatively high aeration intensity of 8 min aeration and 2 min intervals as a cycle with an aeration rate of 0.5 m^3/min had been consistently maintained. We monitored DO changes at each sampling site within one aeration cycle (Fig. S1). It can be observed that the DO concentration in car1 was close to susp, both below 0.5 mg/L. Comparatively, car2 and car3 exhibited notably higher average DO, reaching 2.16 and 1.45 mg/L, respectively. The NH_4^+-N contents in the carrier layer of the three sampling sites were close. As for NO_2^--N, susp and car1, being at the forefront of flow, reached much higher levels of 105.58 and 86.72 mg/L average, respectively, compared to car2 and car3. On the contrary, NO_3^--N demonstrated the opposite trend, with susp and car1 showing lower levels than car2 and car3.

3.2. SAAs at different DO exposure levels

The photos of the sponge cubes and Pall rings collected in our reactor are presented in Fig. S2, from which it is readily apparent that the red biofilm on both the sponge cubes and the Pall rings was predominantly distributed on the surface, while the cross-section revealed a dark brown colour in the interior. This indicated that anammox bacteria primarily inhabited the surface of the carriers. Accordingly, the DO concentration in the liquid phase can be considered the actual concentration exposed to the anammox bacteria within the carrier biofilm. Based on it, the SAA of each sample was tested at different levels of DO exposure, as shown in Fig. 3. Noticeably, under anaerobic and low-DO conditions, the SAA of suspended sludge was conspicuously higher than that of the other samples from the carrier layer. The highest SAA was obtained at a shaker speed of 50 rpm, reaching 6.23 mg-N/(g-MLVSS·h), with a DO range of 1.09 ± 0.17 mg/L. The SAA of susp decreased sharply as the DO concentrations increased. However, DO exposure did not have a noteworthy impact on the anammox activity of the carriers, with the SAAs remaining at 3~4 mg-N/(g-MLVSS·h). The slope of the linear regression of each sample (as shown in the small window in Fig. 3) indicated that the suspended sludge was more sensitive to DO change than the biomass in the carriers.

3.3. Microbial community

Based on metagenomic sequencing, the microbial community structures of sample susp, spon, and pall were obtained (Fig. 4). At the phylum level, the three most abundant phyla were *Proteobacteria, Chloroflexi*, and *Planctomycetota*, accounting for 29.55 %, 26.68 %, and 13.17 % of the total abundance across all samples, respectively. Among them, the abundance of *Planctomycetota* in suspended sludge, sponge cubes, and Pall rings was 15.31 %, 10.94 %, and 13.18 %, respectively. At the genus level, the functional anammox bacterium *Ca. Kuenenia* was the most abundant genus across all samples, while AOB, another important functional microorganism in the CANON reactor, primarily belonged to the genus *Nitrosomonas*. Other detected functional microbes, such as the anammox bacteria *Ca. Brocadia, Ca. Anammoximicrobium*, the AOB *Nitrosococcus, Nitrosospira*, as well as the nitrite-oxidizing bacteria (NOB) *Nitrobacter, Nitrospira*, which were not expected to be present in the CANON reactor, had abundances below 0.1 % in all samples and are not shown in Fig. 4. Therefore, *Ca. Kuenenia* and *Nitrosomonas* in suspended sludge and carriers were the main focus. Both of them exhibited the highest abundance in suspended sludge, with *Ca. Kuenenia* reaching 11.87 %, and *Nitrosomonas* accounting for 7.48 %. Their abundances in sponge cubes were close, with the former at 4.63 % and the latter at 4.89 %. However, the Pall rings had a significant difference, with *Ca. Kuenenia* reaching 9.03 % compared to only 1.86 % for *Nitrosomonas*.

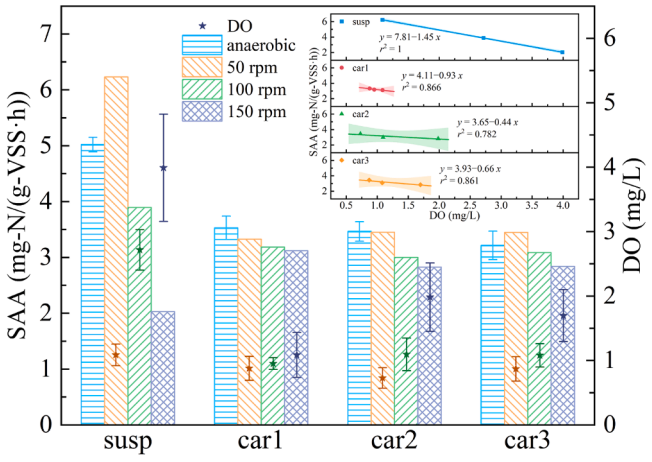

Fig. 3. SAAs at different DO exposure levels. The attached plot is the linear regression of SAA to dissolved oxygen.

3.4. Metatranscriptomics to reveal the expression of Ca. Kuenenia

All genes expressed by *Ca. Kuenenia* in each sample were annotated using the KEGG database. A total of 1157 annotations were acquired. Partial least squares-discriminant analysis (PLS-DA) (Fig. S3) showed that sample susp was far from the other samples, while car2 and car3 clustered. The gene expression differential analysis compared susp as a control and carrier samples (Fig. S4). Samples car2 and car3 had much more DEGs and exhibited a greater diversity of enriched differential metabolic pathways (more detailed information is described in Text S5). Overall, the DEGs in carrier samples were primarily enriched in modules or pathways related to carbon metabolism, biosynthesis of cofactors, and bacterial secretion system (Fig. S5). For example, carbon fixation, TCA cycle, cysteine synthesis, belonging to the carbon metabolism, thiamine synthesis, heme synthesis, belonging to the biosynthesis of cofactors, and protein export belonging to the bacterial secretion system were highly enriched.

From the differential fold change heatmap (Fig. 5(A2)(B2)(C2)), consistent trends in the regulation of DEGs were observed in all carrier samples despite exhibiting varying fold changes. Fig. 5(A) illustrates the expression differences of genes involved in central carbon metabolism by *Ca. Kuenenia*. It was evident that most of the genes in the carrier samples showed a downregulation trend, including modules such as the Wood-Ljungdahl pathway, EMP pathway, TCA cycle, and cysteine synthesis. As for the fold changes in gene expression, car2 and car3 exhibited prominent differences compared to susp, resulting in most genes being identified as DEGs. However, car1 had no identified DEGs due to the fold change not reaching the threshold ($|\log_2 FC| < 1$). The DEGs involved in the biosynthesis of cofactors were mainly distributed in modules related to the synthesis of coenzyme A (CoA), heme, cobalamin, thiamine, and menaquinone (Fig. 5(B)). It is noticeable that the synthesis of CoA and thiamine showed a significant downregulation trend, while heme and cobalamin exhibited the opposite. It was particularly noteworthy that the gene *wrbA*, encoding menaquinone oxidoreductase, significantly upregulated in all carrier samples, especially in car2 and car3, where the fold changes exceeded fivefold. The synthesis of glycerophospholipids, including phosphatidylserine, cephalin, lecithin, phosphatidylglycerophosphate, and phosphatidylglycerol, showed a downregulation trend (Fig. 5(C)). Regarding protein secretion, we only detected the expression of genes related to the type II bacterial secretion system by *Ca. Kuenenia*. The relevant genes encoding signal recognition particle (SRP) receptor protein sec*DF*, twin-arginine translocase protein *tatA*, and type II secretion inner membrane protein *gspK* upregulated.

3.5. Correlation analysis

Multiple statistical methods were employed to investigate the

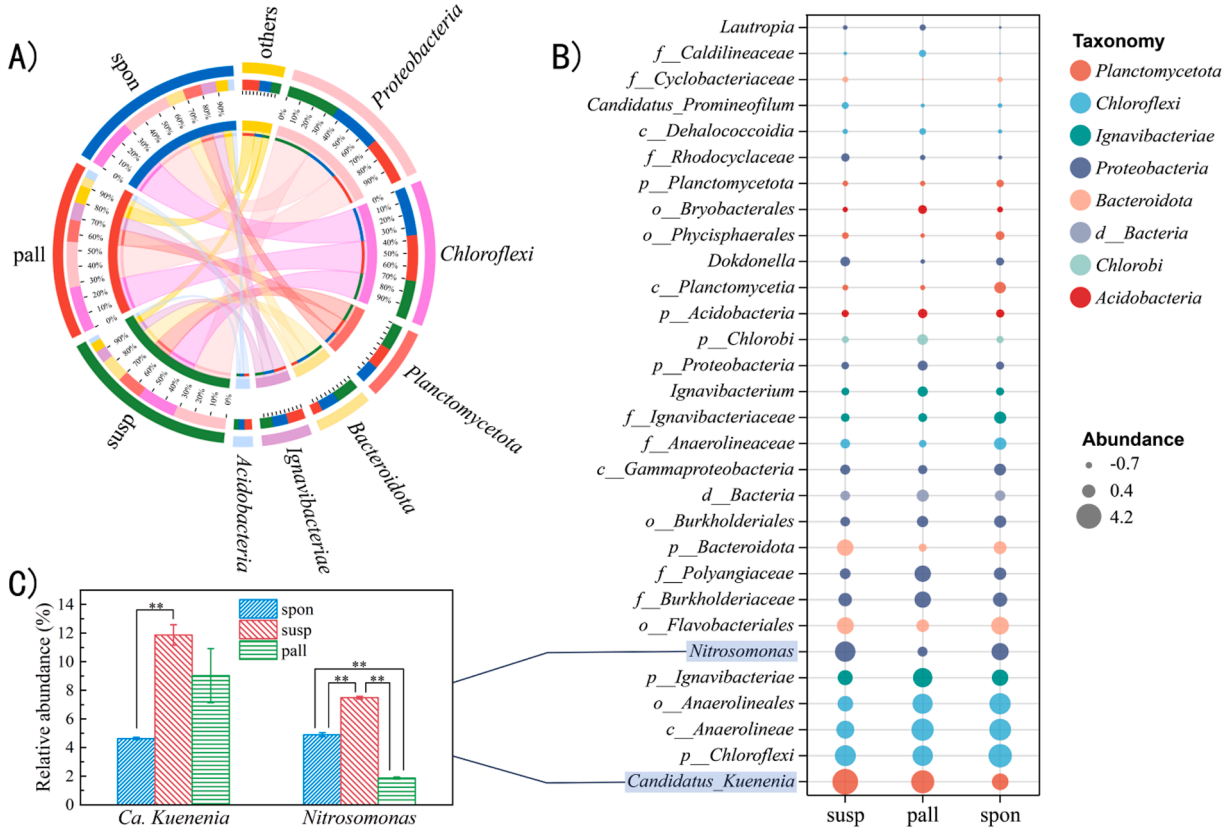

Fig. 4. Microbial community structures of suspended sludge (susp), sponge cubes (spon), and Pall rings (pall): Distribution at the level of phylum (A), genera (B), and relative abundances of *Ca. Kuenenia* and *Nitrosomonas* (C).

distribution patterns of DEGs in *Ca. Kuenenia* and the driving factors behind their differential expression. Redundancy analysis (RDA) was conducted on the expression levels of DEGs and the environmental factors in each sample, as depicted in Fig. 6(A). The results indicated that the genes most strongly influenced by environmental factors were those associated with oxygen detoxification and heme biosynthesis. The potential genes involved in oxygen detoxification, including non-heme chloroperoxidase *cpo*, catalase *katE*, menaquinone oxidoreductase *wrbA*, as well as heme biosynthesis-related genes Fe-coproporphyrin III synthase *ahbC* and porphobilinogen synthase *hemB*, exhibited a highly positive correlation with DO. Besides, Spearman correlation analysis (Fig. 6(B)) showed that most carbon metabolism-related genes showed a significant negative correlation with DO and a significant positive correlation with NO_2^--N. A similar trend also existed in glycerophospholipid synthesis. CoA and thiamine exhibited a negative correlation with DO in the biosynthesis of cofactors, while heme and cobalamin displayed the opposite. Additionally, the potential genes for oxygen detoxification, except for the ubiquinol-cytochrome c reductase gene *CYTB* and *cbb3*-type cytochrome c oxidase gene *ccoNO* involved in oxidative phosphorylation, were positively correlated with DO. As illustrated in Fig. 6 (C), a co-occurrence network of the DEGs was constructed. It was observed that a topological module was formed by the co-occurrence of genes related to carbon metabolism, CoA synthesis, glycerophospholipid synthesis, certain type II secretion system genes, and genes *CYTB* and *ccoNO*. Another major module was formed by the genes related to heme synthesis, another set of the type II secretion system genes, potential genes for oxygen detoxification (*SOD2, katE, dfx, cpo*, etc.), and the menaquinone oxidoreductase gene *wrbA*.

4. Discussion

4.1. DO resistance

DO was usually controlled at low level in CANON systems to achieve good performances of nitrogen removel. One study observed that DO above 1.15 mg/L led to rapid deterioration in a pilot-scale single-stage PN/A reactor, suggesting that high concentrations of DO have a decisive destructive effect on single-stage PN/A systems (Yang et al., 2016). This effect was attributed to the direct inhibition of anammox and the promotion of NOB proliferation, leading to the competition for substrate nitrite. Therefore, most pilot-scale studies maintained DO at lower levels to achieve the desired nitrogen removal loads. For example, Kim et al. (2022) achieved a TN removal load of 220 ± 10 g-N/m^3/d by controlling DO below 0.1 mg/L. Liang et al. (2016) introduced polyethene sponge cubes as carriers for anammox biofilms, achieving an average TN removal load of 506 g-N/m^3/d but still requiring strict control of DO below 0.5 mg/L. In comparison, in this study, the average TN removal load during the stable phase (Phase II) reached 428 g-N/m^3/d, which was not lower than the reported values in previous pilot studies. Moreover, the maximum TN removal load of 1096 g-N/m^3/d exceeded the performance of previous studies (Kim et al., 2022; Liang et al., 2016; Yang et al., 2016). The ratio of COD/N in the mature leachate in this study was 0.74 ± 0.11 hence the heterotrophic denitrification was considered to affect the nitrogen removal less. Accordingly, the high-intensity aeration adopted to promote partial nitrification in our study did not affect the nitrogen removal efficiency of anammox.

The average DO concentrations at sampling sites 2 and 3 reached 2.16 and 1.45 mg/L, respectively, much higher than the traditionally recognized inhibitory levels for anammox (Varas et al., 2015). More remarkably, in our CANON reactor, anammox biofilms were distributed on the carriers' surface (Fig. S2), directly exposed to the oxygen-rich

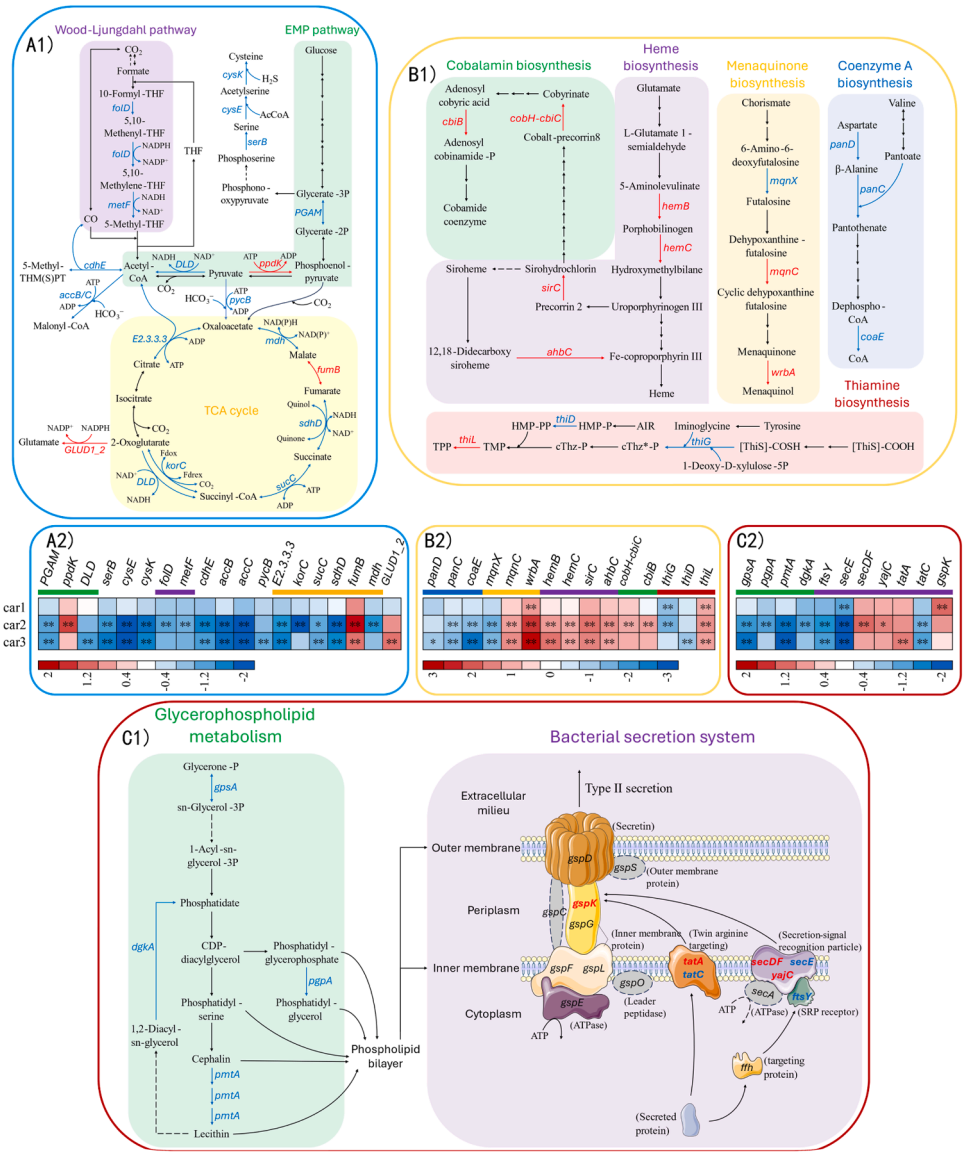

Fig. 5. Differential metabolic pathways of *Ca. Kuenenia*: (A) carbon metabolism; (B) biosynthesis of cofactors; (C) Glycerophospholipid metabolism and bacterial secretion. The following number "1″ identifies the pathway map, and "2″ identifies the heat map of the fold changes. Up- and down-regulated DEGs are marked in red and blue, respectively. The dotted line indicates that the gene was not detected. Asterisks on the heat map indicate significant differences, *: $|\log_2 FC| > 1$ and p-adj < 0.05, **: $|\log_2 FC| > 1$ and p-adj < 0.01.

liquid phase. It contradicted the conventional common sense of biofilm stratification primarily driven by oxygen concentration gradients. Furthermore, microbial community analysis revealed that the relative abundance of NOB in both suspended sludge and carriers was less than 0.1 %, indicating no abnormal NOB proliferation due to high DO. Anammox bacteria still maintained an absolute advantage in the competition for substrate nitrite. These observations imply that the anammox biofilms on the carriers exhibited DO resistance.

The batch tests have provided more visually compelling evidence for the DO resistance. The decline in SAA with the rising DO was minimal in the carrier samples, whereas the suspended sludge demonstrated an apparent inhibition. It was confirmed that anammox bacteria distributed on the carriers' surface possessed more robust resistance to DO than the suspended sludge. This observation aligned with our previous inference based on the operational conditions of the pilot-scale reactor. Although anammox activity in suspended sludge was more prone to be suppressed by DO, it exhibited higher anammox rates under anaerobic or low-oxygen conditions (Fig. 3). The abundance of anammox bacteria (mainly *Ca. Kuenenia* in this study) in the suspended sludge was higher than in the sponge cubes and Pall rings (Fig. 4). This finding contradicted the majority of previous studies, where anammox biofilms or granular sludge typically exhibit higher nitrogen removal efficiency and anammox bacteria abundance than suspended floc-like sludge (Liu et al., 2020). It is worth mentioning that, despite the higher abundance of anammox bacteria in the suspended sludge, the carrier layer remained the main contributor to TN removal within the reactor due to higher total biomass. Based on estimates of biomass and SAA, the contributions to TN removal from the suspended sludge layer and carrier layer were 2030 g-N/d and 9187 g-N/d, respectively, with a ratio of 18.1 %: 81.9 %. Detailed calculation procedures are provided in Text S6.

When DO was not a limiting factor, the substrate (nitrite) gradient would become the primary determinant of the hierarchical distribution of the biofilm (Feng et al., 2022). Due to suboptimal partial nitrification activity, prolonged high-intensity aeration and additional nitrite supplementation had been implemented in this CANON process. The suspended sludge resided at the forefront of flow (Fig. 1), where the substrate was most abundant. Meanwhile, when the substrate nitrite reached the carrier layer, where competition for substrate was

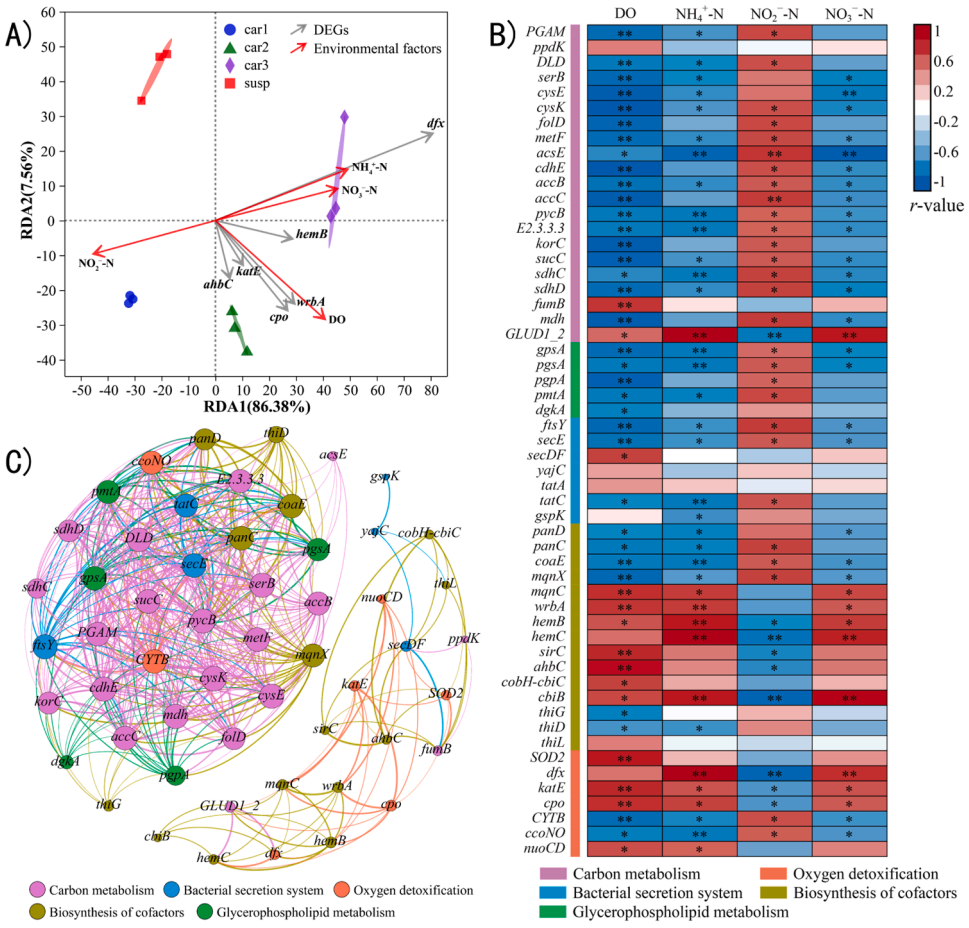

Fig. 6. Correlation analysis of DEGs in *Ca. Kuenenia*: (A) RDA of DEGs and environmental factors. Considering the aesthetics of the image, only the top six DEGs that are most affected are shown in the figure. (B) Heat map of Spearman correlation between DEGs and environmental factors. *: $p < 0.05$, **: $p < 0.01$. (C) Co-occurrence network of the DEGs. The threshold is Spearman correlation coefficient > 0.7 and $p < 0.05$.

intensified due to higher biomass, it had already been depleted to a considerable extent. Besides, the higher abundance of AOB in the suspended sludge accelerated oxygen consumption, resulting in a lower DO level than the carrier layer (Fig. 2(B)). Considering the above, we believe the combined effects of DO and substrate availability have shaped the unique ecological distribution of anammox bacteria in this CANON process. Specifically, the suspended sludge layer held the richer substrate and lower DO, thus promoting a higher abundance of anammox bacteria. In contrast, for the carrier layer, a decision-making algorithm that has evolved spontaneously in anammox bacteria, enabling them to optimize their survival under challenging conditions. The substrate nitrite was relatively insufficient for the carriers, leading anammox bacteria to primarily settle in the outer layer of the biofilm. This positioning allowed them to efficiently capture the limited substrate despite direct exposure to high DO levels, thereby enhancing their oxygen tolerance. Furthermore, studies have shown that *Ca. Kuenenia* is a *K*-strategist microbe, while *Ca. Brocadia* belongs to the *r*-strategist category (Zhang et al., 2019). The former possessing better oxygen resistance and substrate affinity than the latter (Oshiki et al., 2016; Zhang et al., 2017). As a result, *Ca. Kuenenia* was more adaptable to the environmental conditions within this reactor and became the dominant.

4.2. Regulation of metabolism as a survival strategy for oxygen stress

Metatranscriptomics provided a practical approach to uncovering the intrinsic microscale mechanisms underlying the oxygen tolerance and detoxification capabilities of *Ca. Kuenenia*. Due to the relatively similar environmental conditions (Fig. 2(B)), fewer DEGs were identified between car1 and susp. By comparison, the gene expression between car2 and car3 was highly similar but significantly different from susp (Fig. S3). Subsequently, metabolic pathways, which were highly enriched by DEGs and of meaningful physiological significance for *Ca. Kuenenia*, were selected for further in-depth analysis.

Carbon metabolism, as the foundation of all life activities, is the most representative indicator of the overall metabolic level of organisms. As autotrophs, anammox bacteria fix carbon through the Wood-Ljungdahl pathway (Strous et al., 2006), in which the gene expression of *Ca. Kuenenia* on the carriers was downregulated (Fig. 5(A)), indicating decreased autotrophic metabolic activity. Additionally, the expressions of most genes related to EMP pathway and TCA cycle, which serve as the prime sources of ATP, were also downregulated, suggesting a comprehensive reduction in energy metabolism levels. Previous studies have observed a global transcriptional downregulation of central carbon metabolism in *Ca. Kuenenia* exposed to DO, which was believed to favor its survival under DO inhibition (Yan et al., 2020). Our study similarly discovered an intensely negative correlation between the gene expression of *Ca. Kuenenia*'s carbon metabolism and DO (Fig. 6(B)), implying that the lower energy metabolism level may be one of the reasons why the anammox activity of carrier samples was less inhibited under intense DO exposure. However, insufficient evidence still hindered an exhaustive explanation of why downregulation of carbon metabolism became a strategy for *Ca. Kuenenia* to cope with DO exposure. It is known that continuous electron transfer during ATP production in the respiratory chain can easily lead to electron leakage, and oxygen readily combines with these leaked electrons to form superoxide radicals, which further generate other reactive oxygen species (ROS) and damage cellular

structures (Shimizu and Matsuoka, 2019). Since carbon metabolism is a primary source of ATP, a significant amount of ROS will most likely be produced when oxygen is present. Hence, we speculate that the downregulation of carbon metabolism to reduce ROS generation is a protective mechanism for *Ca. Kuenenia* in response to oxidative stress.

Regarding the electron carriers in the respiratory chain, quinone pool, it was worth noting that the expressions of multiple genes involved in ubiquinone (coenzyme Q) synthesis were not detected in *Ca. Kuenenia* despite the expression of ubiquinone reductase gene *nuoCD*. In contrast, the genes involved in menaquinone synthesis were fully expressed, and the gene encoding menaquinone oxidoreductase, *wrbA*, was highly upregulated in the carrier samples (Fig. 5(B)) and showed a strong positive correlation with DO (Fig. 6). Some scholars have pointed out that for Gram-negative bacteria, obligate anaerobes and aerobes exclusively consisted of naphthoquinones, which menaquinone belongs to, and ubiquinones, respectively (Collins and Jones, 1981). Menaquinone oxidoreductase is responsible for the reduction of menaquinone (MQ) to menaquinol (MQH_2, the reduced form of menaquinone), which prevents the interaction of menasemiquinone ($MQH^{\cdot-}$) with oxygen, thereby militating the generation of superoxides (Patridge and Ferry, 2006). It was reported that menaquinone oxidoreductase was active in *E. coli* when it grew in hyperoxic environments and was consistent with superoxide dismutase and catalase (Anand et al., 2019). Hence, it was reasonable to believe that *Ca. Kuenenia* similarly prevented the generation of superoxide radicals by upregulating the expression of the gene *wrbA*.

The biosynthesis of other cofactors, such as CoA, cobalamin, and thiamine, was also consistent with the regulation of carbon metabolism. A detailed discussion about them is given in Text S7. However, heme synthesis was significantly upregulated. Heme plays a crucial role in the physiological activities of anammox bacteria. It not only serves as the active centre for key enzymes involved in anammox process (such as nitrite reductase NirS, hydrazine synthase HZS, hydrazine dehydrogenase HDH, etc.) (Kartal and Keltjens, 2016) but also acts as a common component of various oxidative-reductive proteins involved in oxygen detoxification (such as catalase, cytochrome c peroxidase, etc.) (Poulos, 2014). In this study, we observed the gene upregulations of hydrazine dehydrogenase HDH and catalase in *Ca. Kuenenia*. The upregulation of heme synthesis may have vital implications in maintaining anammox activity under high-oxygen conditions.

Glycerophospholipids, as the predominant constituents of cell membranes, directly impact the synthesis of phospholipid bilayers. Bacterial growth is also closely linked to the accumulation of cell membrane lipids (Zhang and Rock, 2008). Therefore, the synthesis of glycerophospholipids represents a crucial metabolic pathway that reflects bacterial cell growth and proliferation (Tang et al., 2018). Consistent with the downregulation of central carbon metabolism, the synthesis of glycerophospholipids decreased across the board (Fig. 5 (C)). This indicated a deceleration in the growth and proliferation of *Ca. Kuenenia* on the carriers. However, the expression of specific genes related to type II secretion in the bacterial secretion system was observed to be upregulated (Fig. 5(C)), implying an enhancement in the release of certain extracellular proteins. Numerous Gram-negative bacteria utilize a complex type II secretion system to transport diverse proteins from the periplasm across the outer membrane to the extracellular milieu (Korotkov et al., 2012). Jia et al. (2021) found that the abundance of genes related to type II secretion was positively correlated with that of anammox bacteria. These bacteria might therefore employ this pathway for the secretion of EPS proteins. Additionally, Liao et al. (2019) observed a significant upregulation in the expression of genes related to type II secretion in *E. coli* when exposed to high concentrations of CO_2 that induced the production of a substantial amount of ROS. Studies have noted that proteins in EPS can alleviate the toxicity of H_2O_2 to microorganisms by sacrificing themselves through reaction (Jiang et al., 2022). Accordingly, we speculated that enhancing the release of specific extracellular proteins through the type II secretion system may also be one of the strategies employed by *Ca. Kuenenia* in response to oxidative stress. Quantification of EPS showed that the carrier samples had higher levels of both total EPS and protein content compared to the suspended sludge sample (Fig. S6). This result to some extent supported our hypothesis that extracellular proteins were involved in the oxygen resistance of anammox bacteria.

The co-occurrence network revealed two main topological modules (Fig. 6(C)) that exhibited different regulation trends of the DEGs, which provided us with a global perspective on the metabolic regulation of *Ca. Kuenenia* in response to DO exposure: enzymes and cofactors involved in carbon metabolism and oxidative phosphorylation were downregulated, reducing the energy metabolism level to minimize the generation of ROS. Particularly, the menaquinone oxidoreductase was upregulated to further reduce the formation of superoxide radicals by preventing the leaked electrons from combining with oxygen. The glycerophospholipids synthesis was subsequently downregulated, leading to a slowdown in cell growth and proliferation. Simultaneously, the secretion of certain extracellular proteins was enhanced probably to alleviate the ROS by sacrificing themselves.

4.3. Oxygen detoxification pathway for Ca. Kuenenia

A potential set of genes related to oxygen detoxification was selected from the 388 DEGs in this study. Their expression levels in each sample were analyzed and correlations were examined (Fig. 6), based on which a putative oxygen detoxification pathway for *Ca. Kuenenia* was proposed, as shown in Fig. 7. Superoxide dismutase and catalase are the enzymes most commonly responsible for sequentially reducing superoxide radicals to H_2O_2 and H_2O in aerobic cells (Cannio et al., 2000). This study found that *Ca. Kuenenia* expressed the superoxide dismutase gene *SOD2* and the catalase gene *katE*, which was consistent with the findings of Yan et al. (2020). Moreover, the expression of both genes was upregulated in the carrier samples and exhibited a significant positive correlation with DO, indicating their involvement in oxygen detoxification. Superoxide reductase can use rubredoxin as a substrate to convert superoxide radicals into H_2O_2 (Jenney et al., 1999). The gene *dfx*, encoding superoxide reductase, was also differentially expressed by *Ca. Kuenenia* and had much higher expression levels than *SOD2* (Fig. 7), suggesting that superoxide reductase *dfx* may play a more central role in the conversion of superoxide radicals to H_2O_2 in *Ca. Kuenenia*. Interestingly, Ji et al. (2019) found the opposite situation in *Ca. Brocadia*, where the expression of *SOD2* was higher than that of *dfx*, demonstrating different choices of oxygen detoxification pathways between *Ca. Brocadia* and *Ca. Kuenenia*. In addition, to the best of our knowledge, there have been no reports on the expression of the non-heme chloroperoxidase gene *cpo* in anammox bacteria. Non-heme chloroperoxidase can utilize H_2O_2 to oxidize hydrocarbons into halogenated hydrocarbons (Manoj, 2006). In this study, the gene *cpo* was also observed to be upregulated in the carrier samples and exhibited a significant positive correlation with DO, implying its participation in H_2O_2 reduction.

Strikingly, among the potential oxygen detoxification genes, the genes *ccoNO* and *CYTB* showed opposite trends (Fig. 6). Yang et al. (2022) suggested that the *cbb3*-type cytochrome c oxidase encoded by the gene *ccoNO* conferred strong oxygen tolerance to their newly discovered anammox genus, "Ca. Loosdrechtia aerotolerans". However, in this study, the expression of *ccoNO* in *Ca. Kuenenia* was downregulated in the carrier samples and negatively correlated with DO. We proposed that the *cbb3*-type cytochrome c oxidase did not participate in the oxygen detoxification of *Ca. Kuenenia* but retained its original role in oxidative phosphorylation, thus exhibiting expression trends consistent with carbon metabolism. The same reasoning applied to the gene *CYTB*, encoding cytochrome c reductase, which was believed to be involved in oxygen detoxification of *Ca. Brocadia* by Ji et al. (2019). These observations implied that anammox bacteria may exhibit rich diversity in their choices of oxygen detoxification pathways. Based on the above, a hypothesis for the oxygen detoxification pathway of *Ca. Kuenenia* was

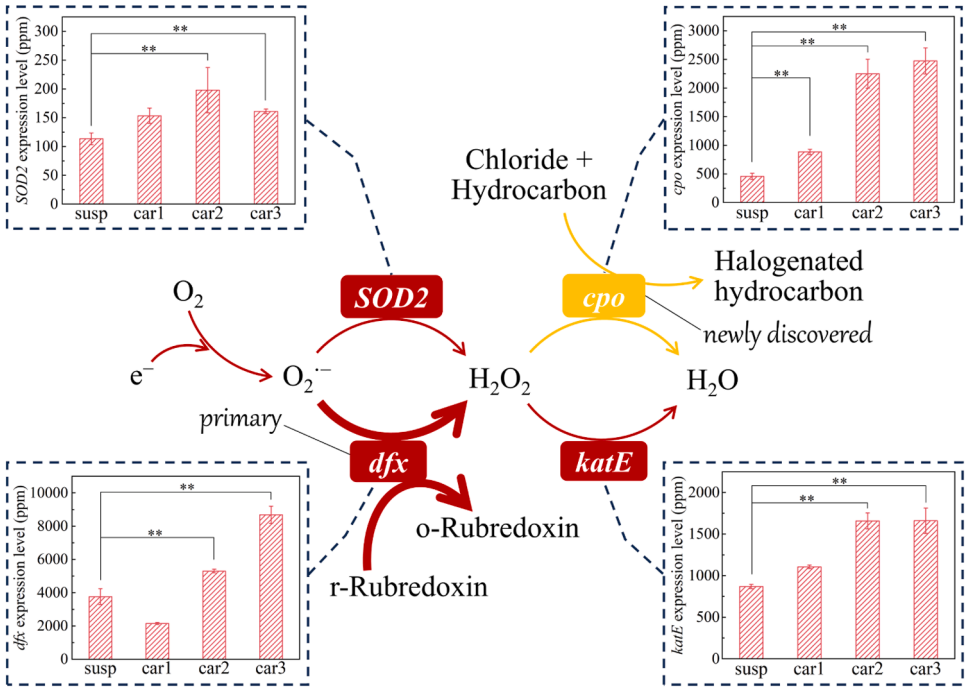

Fig. 7. The proposed hypothesis of the oxygen detoxification pathway and the expression levels of corresponding genes in each sample. To highlight the particularity of oxygen detoxification in *Ca. Kuenenia*, the *dfx* and *cpo* processes are shown in bold and gold, respectively.

proposed: superoxide radicals were initially converted to H_2O_2 by superoxide dismutase *SOD2* and superoxide reductase *dfx*. Due to the higher gene expression, *dfx* might play a major role in superoxide radicals conversion, where the reduced rubredoxin (r-Rubredoxin) was converted to its oxidized form (o-Rubredoxin) to provide electrons. H_2O_2 was then reduced to H_2O through the actions of non-heme chloroperoxidase *cpo* and catalase *katE*. Hydrocarbons were probably the electron source for the *cpo* process. The expressions of genes involved in oxygen detoxification were upregulated to eliminate ROS and alleviate oxidative stress.

5. Conclusions

This study demonstrated that the anammox bacteria, distributed in the suspended sludge and carrier-based biofilm in the pilot-scale CANON reactor, exhibit varying degrees of resistance to DO exposure. Metatranscriptomics confirmed that *Ca. Kuenenia* responds to oxygen stress with changes in gene expression across various metabolic pathways, which endows it with oxygen tolerance and detoxification capabilities beyond the traditional understanding that DO inhibits anammox activity. We identified a novel oxygen detoxification pathway that differs from those reported in other anammox species, suggesting that different adaptive strategies may be employed by anammox bacteria when encountering DO exposure in their environment. Moreover, these findings have pratical implications for field applications. For example, the DO levels in a full-scale CANON reactor are not uniform but fluctuate, which is a key factor inhibiting anammox bacteria. If anammox bacteria can develop capacities for oxygen tolerance and detoxification, the field application of CANON technology is applicable to a wider range of DO environments, potentially reducing the need for stringent control of operational parameters. Admittedly, the threshold DO level that anammox bacteria could endure over the long term need to be thoroughly investigated. This study significantly advances our understanding of the physiological characteristics of anammox bacteria and provide a profound theoretical foundation for constructing efficient and stable integrated autotrophic nitrogen removal processes.

CRediT authorship contribution statement

Huaihao Xu: Writing – original draft, Visualization, Methodology, Investigation. **Xiaojun Wang:** Writing – review & editing, Visualization, Supervision, Funding acquisition, Formal analysis. **Mingyuan Wang:** Methodology, Investigation, Data curation. **Junbin Wu:** Investigation. **Bo Zhang:** Methodology. **Jinsong Wang:** Writing – review & editing. **Qiuting Zhang:** Project administration, Methodology. **Bingrong Lin:** Project administration. **Shaohua Chen:** Writing – review & editing, Supervision, Conceptualization.

Declaration of competing interest

The authors declare that they have no known competing financial interests or personal relationships that could have appeared to influence the work reported in this paper.

Acknowledgements

This research was financially supported by the Science and Technology Program of Fujian Province (3502ZCQXT2021011) and the National Natural Science Foundation of China (51708536).

Supplementary materials

Supplementary material associated with this article can be found, in the online version, at doi:10.1016/j.watres.2024.122613.

Data availability

Data will be made available on request.

References

Altschul, S.F., Madden, T.L., Schaffer, A.A., Zhang, J.H., Zhang, Z., Miller, W., Lipman, D. J., 1997. Gapped BLAST and PSI-BLAST: a new generation of protein database search programs. Nucleic. Acids. Res. 25 (17), 3389–3402.

Anand, A., Chen, K., Yang, L., Sastry, A.V., Olson, C.A., Poudel, S., Seif, Y., Hefner, Y., Phaneuf, P.V., Xu, S., Szubin, R., Feist, A.M., Palsson, B.O., 2019. Adaptive evolution reveals a tradeoff between growth rate and oxidative stress during naphthoquinone-based aerobic respiration. Proceed. Nat. Acad. Sci. 116 (50), 25287–25292.
APHA, AWWA and WEF, 2012. Standard methods for the examination of water and wastewater. American Public Health Association, Washington, DC.
Cannio, R., Fiorentino, G., Morana, A., Rossi, M., Bartolucci, S., 2000. Oxygen: friend or foe? Archaeal superoxide dismutases in the protection of intra- and extracellular oxidative stress. Front. Biosci. 5, D768–D779.
Collins, M.D., Jones, D., 1981. Distribution of isoprenoid quinone structural types in bacteria and their taxonomic implication. Microbiol. Rev. 45 (2), 316–354.
Du, R., Li, C., Liu, Q.T., Fan, J., Peng, Y.Z., 2022. A review of enhanced municipal wastewater treatment through energy savings and carbon recovery to reduce discharge and CO2 footprint. Bioresour. Technol. 364, 12.
Feng, Y., Wu, L., Zhang, Q., Li, X., Wang, S., Peng, Y., 2022. Double anammox process in the AOAO process of treating real low C/N sewage: validation, enhancement, and quantification of the contribution of anammox in the oxic zone. Sci. Total. Environ. 849, 157866.
Jenney, F.E., Verhagen, M., Cui, X.Y., Adams, M.W.W., 1999. Anaerobic microbes: oxygen detoxification without superoxide dismutase. Science 286 (5438), 306–309.
Ji, X., Wu, Z., Sung, S., Lee, P.H., 2019. Metagenomics and metatranscriptomics analyses reveal oxygen detoxification and mixotrophic potentials of an enriched anammox culture in a continuous stirred-tank reactor. Water. Res. 166.
Jia, F., Peng, Y., Li, J., Li, X., Yao, H., 2021. Metagenomic prediction analysis of microbial aggregation in anammox-dominated community. Water. Environ. Res. 93 (11), 2549–2558.
Jiang, B., Zeng, Q.Z., Hou, Y., Li, H.X., Shi, S.N., Chen, Z.B., Cui, Y.B., Hu, D.X., Ge, H., Che, S., Sui, Y.A., Qi, Y., 2022. The responses of activated sludge to membrane cleaning reagent H2O2 and protection of extracellular polymeric substances. Environ. Res. 203, 10.
Kartal, B., Keltjens, J.T., 2016. Anammox biochemistry: a tale of heme c proteins. Trends. Biochem. Sci. 41 (12), 998–1011.
Kim, J., Yu, J., Kwon, T., Choi, W., Direstiyani, L.C., Jeong, S., Kim, Y., Park, S., Bae, H., Lee, T., 2022. The real-time monitoring system strategy for stable long-term operation of pilot-scale single-stage deammonification (SSD) process treating moderate-strength NH_4^+. J. Water. Process. Eng. 48, 9.
Korotkov, K.V., Sandkvist, M., Hol, W.G.J., 2012. The type II secretion system: biogenesis, molecular architecture and mechanism. Nat. Rev. Microbiol. 10 (5), 336–351.
Liang, Y.C., Daverey, A., Huang, Y.T., Sung, S., Lin, J.G., 2016. Treatment of semiconductor wastewater using single-stage partial nitrification and anammox in a pilot-scale reactor. J. Taiwan. Inst. Chem. Eng. 63, 236–242.
Liao, J., Chen, Y., Huang, H., 2019. Effects of CO(2) on the transformation of antibiotic resistance genes via increasing cell membrane channels. Environ. Pollut. 254 (Pt B), 113045.
Liu, L., Ji, M., Wang, F., Wang, S., Qin, G., 2020. Insight into the influence of microbial aggregate types on nitrogen removal performance and microbial community in the anammox process - A review and meta-analysis. Sci. Total. Environ. 714, 136571.
Manoj, K.M., 2006. Chlorinations catalyzed by chloroperoxidase occur via diffusible intermediate(s) and the reaction components play multiple roles in the overall process. BBA-Proteins Proteomics 1764 (8), 1325–1339.
Montoya-Rosales, J.d.J., Ontiveros-Valencia, A., Esquivel-Hernández, D.A., Etchebehere, C., Celis, L.B., Razo-Flores, E., 2023. Metatranscriptomic analysis reveals the coexpression of hydrogen-producing and homoacetogenesis genes in dark fermentative reactors operated at high substrate loads. Environ. Sci. Technol. 57 (31), 11552–11560.
Mortazavi, A., Williams, B.A., McCue, K., Schaeffer, L., Wold, B., 2008. Mapping and quantifying mammalian transcriptomes by RNA-Seq. Nat. Methods 5 (7), 621–628.
Mulder, A., van de Graaf, A.A., Robertson, L.A., Kuenen, J.G., 1995. Anaerobic ammonium oxidation discovered in a denitrifying fluidized bed reactor. FEMS Microbiol. Ecol. 16 (3), 177–183.
Oshiki, M., Satoh, H., Okabe, S., 2016. Ecology and physiology of anaerobic ammonium oxidizing bacteria. Environ. Microbiol. 18 (9), 2784–2796.
Patridge, E.V., Ferry, J.G., 2006. WrbA from Escherichia coli and Archaeoglobus fulgidus is an NAD(P)H:quinone oxidoreductase. J. Bacteriol. 188 (10), 3498–3506.
Poulos, T.L., 2014. Heme Enzyme Structure and Function. Chem. Rev. 114 (7), 3919–3962.
Ren, S., Wang, Z., Jiang, H., Li, X.Y., Zhang, Q., Peng, Y.Z., 2022. Efficient nitrogen removal from mature landfill leachate in a step feed continuous plug-flow system based on one-stage anammox process. Bioresour. Technol. 347, 10.
Robinson, M.D., McCarthy, D.J., Smyth, G.K., 2010. edgeR: a Bioconductor package for differential expression analysis of digital gene expression data. Bioinformatics. 26 (1), 139–140.
Seuntjens, D., Carvajal-Arroyo, J.M., Ruopp, M., Bunse, P., De Mulder, C.P., Lochmatter, S., Agrawal, S., Boon, N., Lackner, S., Vlaeminck, S.E., 2018. High-resolution mapping and modeling of anammox recovery from recurrent oxygen exposure. Water. Res. 144, 522–531.
Shimizu, K., Matsuoka, Y., 2019. Redox rebalance against genetic perturbations and modulation of central carbon metabolism by the oxidative stress regulation. Biotechnol. Adv. 37 (8), 107441.
Strous, M., Pelletier, E., Mangenot, S., Rattei, T., Lehner, A., Taylor, M.W., Horn, M., Daims, H., Bartol-Mavel, D., Wincker, P., Barbe, V., Fonknechten, N., Vallenet, D., Segurens, B., Schenowitz-Truong, C., Médigue, C., Collingro, A., Snel, B., Dutilh, B. E., Op den Camp, H.J.M., van der Drift, C., Cirpus, I., van de Pas-Schoonen, K.T., Harhangi, H.R., van Niftrik, L., Schmid, M., Keltjens, J., van de Vossenberg, J., Kartal, B., Meier, H., Frishman, D., Huynen, M.A., Mewes, H.W., Weissenbach, J., Jetten, M.S.M., Wagner, M., Le Paslier, D., 2006. Deciphering the evolution and metabolism of an anammox bacterium from a community genome. Nature 440 (7085), 790–794.
Tang, X., Guo, Y., Wu, S., Chen, L., Tao, H., Liu, S., 2018. Metabolomics uncovers the regulatory pathway of acyl-homoserine lactones based quorum sensing in anammox consortia. Environ. Sci. Technol. 52 (4), 2206–2216.
Third, K.A., Sliekers, A.O., Kuenen, J.G., Jetten, M.S.M., 2001. The CANON system (completely autotrophic nitrogen-removal over nitrite) under ammonium limitation: interaction and competition between three groups of bacteria. Syst. Appl. Microbiol. 24 (4), 588–596.
Varas, R., Guzman-Fierro, V., Giustinianovich, E., Behar, J., Fernandez, K., Roeckel, M., 2015. Startup and oxygen concentration effects in a continuous granular mixed flow autotrophic nitrogen removal reactor. Bioresour. Technol. 190, 345–351.
Wang, W.G., Wang, Y.Y., Wang, X.D., Zhang, Y., Yan, Y., 2019. Dissolved oxygen microelectrode measurements to develop a more sophisticated intermittent aeration regime control strategy for biofilm-based CANON systems. Chem. Eng. J. 365, 165–174.
Yan, Y., Wang, W., Wu, M., Jetten, M.S.M., Guo, J., Ma, J., Wang, H., Dai, X., Wang, Y., 2020. Transcriptomics uncovers the response of anammox bacteria to dissolved oxygen inhibition and the subsequent recovery mechanism. Environ. Sci. Technol. 54 (22), 14674–14685.
Yang, Y., Lu, Z., Azari, M., Kartal, B., Du, H., Cai, M., Herbold, C.W., Ding, X., Denecke, M., Li, X., Li, M., Gu, J.D., 2022. Discovery of a new genus of anaerobic ammonium oxidizing bacteria with a mechanism for oxygen tolerance. Water. Res. 226, 119165.
Yang, Y., Zhang, L., Han, X., Zhang, S., Li, B., Peng, Y., 2016. Determine the operational boundary of a pilot-scale single-stage partial nitritation/anammox system with granular sludge. Water. Sci. Technol. 73 (9), 2085–2092.
Zhang, F.Z., Peng, Y.Z., Wang, S.Y., Wang, Z., Jiang, H., 2019. Efficient step-feed partial nitrification, simultaneous Anammox and denitrification (SPNAD) equipped with real-time control parameters treating raw mature landfill leachate. J. Hazard. Mater. 364, 163–172.
Zhang, K., Li, J., Zheng, Z., Zhang, J., Sun, M., Huang, S., 2022. Analyzing the sludge characteristics and microbial communities of biofilm and activated sludge in the partial nitrification/anammox process. J. Water. Process. Eng. 46.
Zhang, L., Narita, Y., Gao, L., Ali, M., Oshiki, M., Ishii, S., Okabe, S., 2017. Microbial competition among anammox bacteria in nitrite-limited bioreactors. Water. Res. 125, 249–258.
Zhang, Y.M., Rock, C.O., 2008. Thematic review series: glycerolipids - Acyltransferases in bacterial glycerophospholipid synthesis. J. Lipid Res. 49 (9), 1867–1874.